SOILS AND FOUNDATIONS Vol. 50, No. 6, 877–892, Dec. 2010
Japanese Geotechnical Society

NUMERICAL METHODS

AKIRA MURAKAMI[i], AKIHIKO WAKAI[ii] and KAZUNORI FUJISAWA[iii]

ABSTRACT

This paper provides a comprehensive survey of the numerical methods related to geotechnical problems, most of which were reported in papers appearing in *Soils and Foundations*. The reason why most of the reviewed papers are concentrated in *Soils and Foundations* is that if we were to include papers appearing in other journals in the field of geotechnical engineering, closely related to numerical methods, e.g., *Computers and Geotechnics*, *Int. J. Numer. Anal. Meth. Geomech.*, etc., we would have to deal with almost all the papers in those journals. Firstly, we present a description of the current status of the numerical methods, and then give a brief review of the literature covering several topics in geotechnical applications. The scope of the review is limited, and thus, the authors do not profess to cover the entire range of literature.

Key words: dynamics, embankment, excavation, FEM, inverse analysis, slope stability (**IGC:** E0/E2/E6/E8)

INTRODUCTION

The developments made in computational capabilities over the last few decades have fostered equally impressive developments in the numerical methods applied to various engineering fields, including geotechnical engineering. Of particular importance is the emergence of the Finite Element Method (FEM) for the solution of geotechnical problems. Recent developments in a nonlinear FEM for soil-water coupled problems, using sophisticated constitutive models, allow us to predict the behavior of soil deposits and structures with high accuracy under static/dynamic loading.

This review does not attempt to include all aspects of the numerical analyses in geotechnical engineering. It focuses on the simulation methods developed as the 'warp' of the overview. The methods are classified into the following categories:

1) Nonlinear FEM under static/dynamic loading
2) Limit theorems: Upper/Lower bound methods and shakedown analysis
3) Limit equilibrium method
4) Micromechanics and DEM
5) Inverse analysis
6) Other methods, i.e., Mesh-free methods, SPH, Finite volume method and so on.

Among the above items, the limit theorems and their applications related to bearing capacity are addressed in another paper entitled 'Foundations', and Micromechanics and DEM are summarized in the paper entitled 'Geomaterial Behavior—Modeling' in this special issue. To facilitate some type of order to the review, the subject matter related to such phenomena can be classified as the 'woof' of the review.

1) Dynamics
2) Slope stability
3) Embankment/Excavation
4) Shear-band formation and localization
5) Foundations related to bearing capacity

Among the items listed above, 'Foundations related to bearing capacity' is reviewed in another paper entitled 'Foundations' in this special issue.

Bold letters denote tensors, vectors or matrices. We explain some notations and symbols used hereafter for tensor calculus. The symbol '$\cdot$' denotes an inner product of two vectors or a single contraction of adjacent indices of any two tensors

$$\left(\text{e.g., } (\boldsymbol{a}\cdot\boldsymbol{b})_i=\sum_j a_{ij}b_j, \quad (\boldsymbol{b}\cdot\boldsymbol{c})_{ijk}=\sum_l b_l c_{lijk}\right).$$

The symbol '$:$' denotes an inner product of a double contraction of adjacent indices of second or higher order tensors

$$\left(\text{e.g., } (\boldsymbol{c}:\boldsymbol{d})_{ij}=\sum_{k,l} c_{ijkl}d_{kl}\right).$$

The symbol '$\otimes$' denotes a dyadic product, e.g., $(\boldsymbol{a}\otimes\boldsymbol{b})_{ijk}=a_{ij}b_k$ for any two vectors or tensors. The notation $\boldsymbol{e}_i$ denotes a set of orthonormal base vectors in a given coordinate system. The symbol '∇' is a vector differential operator which denotes

[i] Professor, Graduate School of Agriculture, Kyoto University, Kyoto, Japan (akiram@kais.kyoto-u.ac.jp).
[ii] Associate Professor, Department of Civil and Environmental Engineering, Gunma University, Kiryu, Japan.
[iii] Lecturer, Graduate School of Environmental Science, Okayama University, Okayama, Japan.
The manuscript for this paper was received for review on September 13, 2010; approved on October 1, 2010.

$$\sum_i \frac{\partial}{\partial e_i} e_i, \quad \text{where} \quad \frac{\partial}{\partial e_i}$$

means the directional differential operator along the vector e_i. When the Cartesian coordinate system is adopted, the positional coordinates are written as

$$x = \sum_i x_i e_i \quad \text{and } \nabla \text{ is described as } \sum_i \frac{\partial}{\partial x_i} e_i.$$

The symbol 'div' denotes the divergence by operating '$\cdot\nabla$' from the right of vectors or tensors

$$\left(\text{e.g., } \operatorname{div} b = b \cdot \nabla = \sum_i \partial b_i / \partial x_i, \quad \operatorname{div} a = a \cdot \nabla = \sum_j \partial a_{ij} / \partial x_j e_i = \nabla \cdot a^T\right).$$

The symbol 'grad' denotes the gradient by operating '∇' for scalars

$$\left(\text{e.g., } \operatorname{grad} a = \nabla a = \sum_i \partial a / \partial x_i e_i\right)$$

or multiplying '$\otimes\nabla$' for vectors and tensors from the right

$$\left(\text{e.g., } \operatorname{grad} b = b \otimes \nabla = \sum_{i,j} \partial b_i / \partial x_j e_i \otimes e_j\right).$$

In this paper, the signs of the stress and the strain components are taken as positive (negative) when they are compressive (tensile).

To save the calculation time, the analytical model with a realistic geometry in 3D is often simplified into the alternative 2D geometry models. Problems, such as the analysis of slopes, retaining walls, and the continuous footings, generally have one dimension very large in comparison with the other two. Hence, if the force and/or applied displacement boundary conditions are perpendicular to, and independent of, this dimension, all cross section will be the same. Such conditions are said to be as plane strain condition, where the stress in a direction perpendicular to the plane of interests is not zero. The strain in the corresponding direction is zero.

On the other hand, axi-symmetric analysis is related to the studies of the stress distributions in bodies of revolution under axi-symmetric loading. For example, a uniform or centrally loaded circular footing, acting on a homogeneous or horizontally layered foundation, has rotational symmetry about a vertical axis through the center of the foundation. Although those 2D approximations offer affordable and economic models, the predicted results are often exaggerated. It is well known that the 3D finite element analysis provides more realistic and accurate results.

NONLINEAR FEM UNDER STATIC/DYNAMIC LOADING

The finite element method (FEM) has long been undoubtedly the most popular, reliable and successful method for numerically simulating the deformation of grounds and structures. Since 1970, *Soils and Foundations* has published more than 130 papers with 'finite element method' among their keywords; these works have helped to make FEM the most feasible numerical method in geotechnical engineering.

FEM is a scheme for numerically solving differential equations; it is suitable for numerical analyses related to elliptic or parabolic partial differential equations. The method discretizes spatially distributed variables, such as displacement, with computational grids called finite elements, and the discretized variables are given at the nodal points of the elements. The basic procedure for FEM is summarized as follows:

1. *Application of the weighted residual method*
   The distribution of the variables within an element is described with approximate functions called shape functions. The weighted residual technique is applied within each element, where shape functions are adopted as the weighting functions. This procedure is known as the Galerkin method; it is repeated for all elements.
2. *Assemblage*
   The equations obtained for each element are assembled into a set of simultaneous linear equations, depending on the geometry of the elements.
3. *Solving the system of linear equations*
   The simultaneous linear equations are then solved with respect to the dicretized variables at the nodal points.

Application of the Weighted Residual Method

Let us take the following equilibrium equation, the fundamental partial differential equation for the static deformation of solids, as an example:

$$\nabla \cdot \sigma + \rho b = \mathbf{0} \tag{1}$$

where

$$\sigma\left(=\sum_{i,j} \sigma_{ij} e_i \otimes e_j\right), \quad b\left(=\sum_i b_i e_i\right)$$

and ρ denote the Cauchy stress tensor, a body force per unit mass and the density of solids, respectively. Stress-strain relationships are needed for solving Eq. (1). For simplicity, the following relation is assumed here:

$$\sigma = c:\varepsilon = \frac{c}{2}:(u \otimes \nabla + (u \otimes \nabla)^T) = c':u \otimes \nabla,$$
$$c'_{ijkl} = \frac{c_{ijkl} + c_{ijlk}}{2} \tag{2}$$

where

$$c\left(=\sum_{i,j,k,l} c_{ijkl} e_i \otimes e_j \otimes e_k \otimes e_l\right),$$
$$c'\left(=\sum_{i,j,k,l} c'_{ijkl} e_i \otimes e_j \otimes e_k \otimes e_l\right),$$
$$\varepsilon\left(=\sum_{i,j} \varepsilon_{ij} e_i \otimes e_j\right) \quad \text{and} \quad u\left(=\sum_i u_i e_i\right)$$

are the material coefficient tensor, the infinitesimal strain

tensor and the displacement vector, respectively. The strain tensor ε in Eq. (2) neglects second-order terms of the finite strain tensor, such as the Green-Lagrangian finite strain tensor and the Almansi finite strain tensor, assuming the inifinitesimal deformation. Symbols i, j, k and l are the positive integers of 1 to 3 in the three-dimensional cases or 1 to 2 in the two-dimensional cases.

Figure 1 shows an example of the numbering of the quadrangular elements and the nodal points. Let the number of elements, the element numbers and the node numbers be denoted by L^e, e and r, respectively, and let $\Gamma(e)$ be a set of node numbers surrounding element e. Taking Fig. 1 as an example, $\Gamma(1)=\{1, 2, 4, 5\}$ is obtained. The displacement vector within an element is approximated into the following function:

$$u^e(x)=\sum_{r\in\Gamma(e)}\tilde{u}^r N^{e,r}(x), \quad 1\le e\le L^e \tag{3}$$

where $u^e(x)$, $\tilde{u}^r$ and $N^{e,r}(x)$ respectively denote the approximate function of the displacement vector defined for the element e, the displacement value at the nodal point r and the shape function related to the nodal point r of the element e, respectively. The elements and the node numbers are consistently expressed as superscripts in this section. Employing the Galerkin method, the following equation is obtained by integrating the governing equation on the domain of an element:

$$\int_{V^e} N^{e,r}(\nabla\cdot\sigma+\rho b)dV=\mathbf{0}, \quad r\in\Gamma(e), \quad 1\le e\le L^e \tag{4}$$

where V and V^e denote volume (or area) and the domain of element e, respectively. With the divergence theorem of Gauss, Eq. (4) is reduced to the following form:

$$\int_{V^e}\nabla N^{e,r}\cdot\sigma dV=\int_{S^e}N^{e,r}n\cdot\sigma dS+\int_{V^e}N^{e,r}\rho b dV \tag{5}$$

where

$$S, \quad S^e \quad \text{and} \quad n\left(=\sum_i n_i e_i\right)$$

denote the boundary area (or length), the boundary sides of element e and the outward unit normal vector at the boundary, respectively. Substituting Eq. (2) into Eq. (5) yields

$$\sum_{q\in\Gamma(e)}\left(\int_{V^e}\nabla N^{e,r}\cdot c'\cdot\nabla N^{e,q}dV\right)\cdot\tilde{u}^q = \int_{S^e}N^{e,r}n\cdot\sigma dS+\int_{V^e}N^{e,r}\rho b dV \tag{6}$$

where q has been introduced to express the node number as well as r. Letting the integrand of the left-hand side be

$${}^qA^{e,r}\left(=\sum_{i,j}{}^qA^{e,r}_{ij}e_i\otimes e_j\right).$$

Equation (6) is rewritten as

$$\sum_{q\in\Gamma(e)}{}^qA^{e,r}\cdot\tilde{u}^q=\int_{S^e}N^{e,r}n\cdot\sigma dS+\int_{V^e}N^{e,r}\rho b dV,$$

$${}^qA^{e,r}=\int_{V^e}\nabla N^{e,r}\cdot c'\cdot\nabla N^{e,q}dV \tag{7}$$

which are linear equations with respect to $\tilde{u}^r(r\in\Gamma(e))$ on element e.

Assemblage

The first term on the left-hand side of Eq. (7) must be determined in order to solve the linear equations. Let the boundary segments or the sides of element e, including a nodal point p, be $S^{e,r}$ (*see* Fig. 2). From the characteristics of the shape functions, the above-mentioned term satisfies the following equation:

$$\int_{S^e}N^{e,r}n\cdot\sigma dS=\int_{S^{e,r}}N^{e,r}n\cdot\sigma dS \tag{8}$$

because the values of the shape functions, $N^{e,r}$, become zero on the remote sides, which do not include nodal point r.

Letting $e\in\Lambda(r)$ be a set of element numbers, including the nodal point r on the boundaries of the elements ($\Lambda(5)=\{1, 2, 3, 4\}$ in Fig. 1, for instance), the following equation holds true unless the nodal point r is located at the global boundary of the computational region:

$$\sum_{e\in\Lambda(r)}\int_{S^e}N^{e,r}n\cdot\sigma dS=\sum_{e\in\Lambda(r)}\int_{S^{e,r}}N^{e,r}n\cdot\sigma dS=\mathbf{0} \tag{9}$$

since the shape functions $N^{e,r}$ are continuous, the outward unit normal vectors n are opposite in direction and σ is assumed to be continuous between adjacent elements.

Taking the summation of Eq. (7), with respect to $e\in\Lambda(r)$, the following equation is obtained with Eq. (8):

$$\sum_{e\in\Lambda(r)}\sum_{q\in\Gamma(e)}{}^qA^{e,r}\cdot\tilde{u}^q=\sum_{e\in\Lambda(r)}\int_{S^e}N^{e,r}n\cdot\sigma dS+\sum_{e\in\Lambda(r)}\int_{V^e}N^{e,r}\rho b dV. \tag{10}$$

This procedure is called assemblage. Unless nodal point r is located at the global boundary, Eq. (10) can be reduced to

$$\sum_{e\in\Lambda(r)}\sum_{q\in\Gamma(e)}{}^qA^{e,r}\cdot\tilde{u}^q=\sum_{e\in\Lambda(r)}\int_{V^e}N^{e,r}\rho b dV \tag{11}$$

with the aid of Eq. (9). When nodal point r is located at the global boundary, the first term on the right-hand side of Eq. (10) is determined by the imposed boundary conditions.

Solving the System of Linear Equations

Equations (10) and (11) are numerically solved by a linear algebraic procedure. If the material coefficient of c or c' is not constant, for example, it depends on the stress, and the stress-strain relationship is not linear, then the nonlinearity requires iterative computation in order to solve the simultaneous equations.

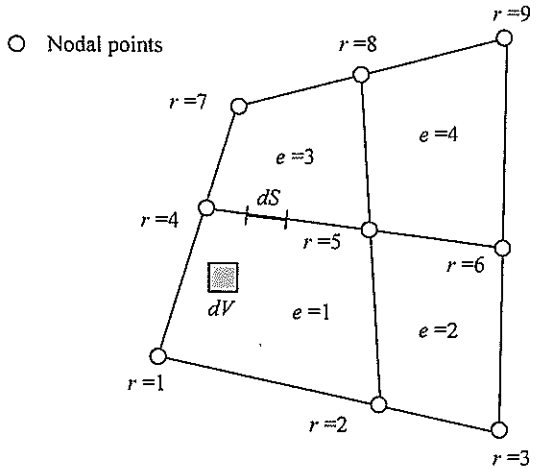

Fig. 1. Example of the numbering of the elements and the nodal points

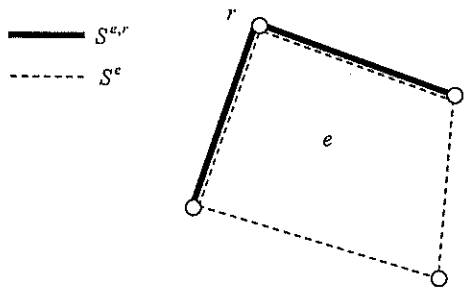

Fig. 2. Definition of the symbols for the element boundary

Soil-water Coupling

Soil consists of soil particles, pore water and pore air, and the aggregation of the soil particles is called the soil skeleton. Soil deformation is related to the stress state of the soil skeleton, which is affected by the flow of pore water and pore air. Therefore, when pore fluids play an important role in the deformation of the soil, the stress state of the soil skeleton needs to be analyzed simultaneously with the flow of pore water and pore air. Supposing the voids of the soil are saturated with water, effective stress σ', defined as the stress exerted onto the soil skeleton, has the following relationship:

$$\sigma = \sigma' - pI \tag{12}$$

where p and

$$I\left(=\sum_{i,j}\delta_{ij}e_i\otimes e_j,\quad \delta_{ij}\text{: Kronecker's delta}\right)$$

denote the pore water pressure and the identity tensor, respectively. Equation (12) is known as the principle of effective stress and stress σ is often called the total stress in soil mechanics. When the coupled problem of the soil skeleton and the pore water is treated, the equation of motion for the soil mass should be described with the effective stress and governing equations must be established for the flow of pore water.

When the static deformation is of interest, the substitution of Eq. (12) reduces Eq. (1) into the following form:

$$\nabla\cdot\sigma' - \nabla p + \rho b = 0 \tag{13}$$

where ρ corresponds to the apparent density of the saturated soil. The effective stress is related to the displacement of the solid (the soil skeleton in this case) via the stress-strain relationship called the constitutive equations.

From the conservation of pore water and Darcy's law, the following equations concerning water seepage are established for the simplest case:

$$\nabla\cdot v' + \nabla\cdot v = 0,\quad v' = -\frac{k}{\rho^f g}(\nabla p + \rho^f b) \tag{14}$$

where

$$v\left(\sum_i v_i e_i = \dot{u}\right),\quad \rho^f,\quad g,\quad v'\left(=\sum_i{}' v_i' e_i\right)$$

and

$$k\left(=\sum_{i,j} k_{ij}e_i\otimes e_j\right)$$

denote the deformation velocity of the solids, the density of the pore water, the magnitude of the gravitational acceleration, the Darcy velocity of the seepage water and the permeability tensor, respectively. Equations (13) and (14) are the governing equations for soil-water coupled problems in static deformation.

Finite Deformation and Constitutive Equations

When we intend to simulate the large deformation of soil, such as in the case of landslides or long-lasting consolidation, computation based on the finite deformation theory is required. The primary difference between infinitesimal (small) and finite (large) deformation concepts lies in whether changes in the configuration of the deforming solids are considered or not. Let us take the linear elastic rod shown in Fig. 3(a) as an example. It is fixed at the extreme left and has an initial length of L_0 and a stiffness of E. Applying compressive stress σ at the extreme right, the rod experiences compressive strain ε and the extreme right is displaced by u_0. From the elastic stress-strain relation, the following equation is obtained:

$$\sigma = E\varepsilon,\quad \varepsilon = u_0/L_0. \tag{15}$$

From Eq. (15), displacement u_0 is calculated as

$$u_0 = \sigma L_0/E. \tag{16}$$

However, if the rod continues to be compressed and the negative stress σ develops in Eq. (16), the absolute value of displacement u_0 will exceed length L_0 when the magnitude of σ becomes greater than E, which is physically unnatural. This result comes from the fact that ε in Eq. (15) does not consider changes in the rod length and that Eq. (16) is based on the infinitesimal deformation concept.

Here, letting increments in σ, ε and u_0 be $\Delta\sigma$, $\Delta\varepsilon$ and Δu_0, respectively, and considering changes in the configuration of the rod, the following equation is established in-

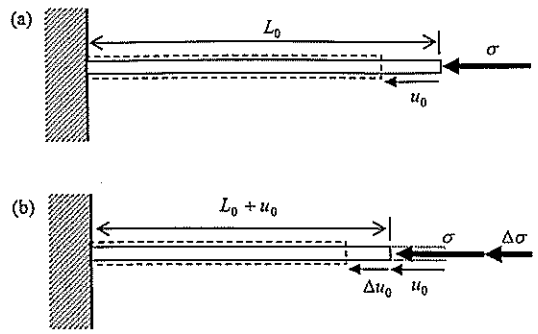

Fig. 3. Illustration of a rod subjected to compressive loading

stead of Eq. (15) by reference to Fig. 3(b):

$$\Delta\sigma = E\Delta\varepsilon, \quad \Delta\varepsilon = \Delta u_0/(L_0+u_0). \tag{17}$$

Equation (17) can be reduced to the following differential equation:

$$\frac{d\sigma}{du_0} = E/(L_0+u_0). \tag{18}$$

Using the condition of $u_0=0$ at $\sigma=0$, the analytical solution for Eq. (18) is given as follows:

$$u_0 = -L_0(1-e^{\frac{\sigma}{E}}) \tag{19}$$

which yields a realistic value for u_0 even if the negative value for compressive stress σ develops. Equation (19) is derived from the concept of finite deformation, which takes into account the alteration of the rod length, with the rate-type stress-strain relationship of Eq. (17). Comparing Eqs. (16) and (19), disregarding changes in the configuration of the rod leads to unrealistic results when the deformation becomes large.

In order to deal with the finite deformation, a stress increment which satisfies the equilibrium condition needs to be determined. In the one-dimensional cases, as explained above, the stress increment is uniform within the rod, so the distribution of the stress increment can be easily calculated. In the two- and three-dimensional cases, the incremental form of the equilibrium equation is derived, as follows, by the material time differentiation of Eq. (1):

$$\nabla\cdot(\dot{\sigma}+(\nabla\cdot v)\sigma+(v\otimes\nabla)\sigma)+\rho\dot{b}=\mathbf{0}. \tag{20a}$$

Further details on the derivation of Eq. (20) can be found in textbooks on continuum mechanics. Using the velocity gradient tensor $L(=v\otimes\nabla)$ and the symbol 'div' and considering the symmetry of the Cauchy stress σ, Eq. (20a) is rewritten as below;

$$\text{div}\,(\dot{\sigma}+(\text{tr}\,L)\sigma+\sigma L^T)+\rho\dot{b}=\mathbf{0}. \tag{20b}$$

When soil-water coupled problems are of interest, Eq. (12) is substituted into Eq. (20) and the water seepage is simultaneously solved. The incremental form for the equation of motion was presented by Noda et al. (2008) for the numerical analyses of the dynamic response of soil. With the aid of constitutive equations, Eq. (20) can be numerically solved with respect to displacement rate v. Then, updating the configuration of solids from the calculated displacements, Eq. (20) is repeatedly solved for the next time step. This procedure is called the updated Lagrangian scheme.

Elasto-plastic or elasto-viscoplastic constitutive equations are often utilized to model soil behavior; they play an important role in solving Eq. (20) because they prescribe the relationship between $\dot{\sigma}$ and v. Asaoka et al. (1997) explained in detail the formulation of an elasto-plastic model to solve the incremental form of the equilibrium equation. Kimoto and Oka (2005) presented an elasto-viscoplastic constitutive model and explained the finite element formulation for the computation of visco-plasticity. The return mapping method is an iteration algorithm used to calculate plastic strain; it is becoming increasingly popular. A detailed procedure for the method is given in Ortitz and Simo (1986) and Simo and Hughes (1998). The theoretical and computational framework of plasticity, based on finite deformation, has been continuously in the process of development over these past decades. The *International Journal of Plasticity* and *Computer Methods in Applied Mechanics and Engineering* are helpful journals for keeping informed of the advancements in this area of research.

As a representative example, a set of governing equations for soil-water coupled problems within finite deformation is listed as follows (*see* Yatomi et al., 1989; Asaoka et al., 1997)

- Equation of equilibrium of forces:

$$\begin{aligned}&\text{div}\,\dot{S}_t+\rho'(\text{tr}\,D)b=\mathbf{0},\\ &\dot{S}_t=\dot{\sigma}+(\text{tr}\,D)\sigma-\sigma L^T\end{aligned} \tag{21}$$

  where L, $D(=(L+L^T)/2)$, $\dot{S}_t$ and b define the velocity gradient, the stretching, the nominal stress rate of the soil skeleton and a constant vector denoting the body force per unit mass, respectively, and the raised dot expresses the material time derivative.

- Effective stress and pore pressure

$$\sigma=\sigma'-pI \tag{22}$$

- Rate type constitutive equation of soil skeleton

$$\hat{T}=L[D] \tag{23}$$

  where $\hat{T}$ denotes, for example, the Green-Naghdi effective stress rate, as shown below

$$\hat{T}=\dot{\sigma}'+\sigma'\Omega-\Omega\sigma', \quad \Omega=\dot{R}R^T \tag{24}$$

  in which Ω and R are the material spin tensor of the solid phase and the rotational tensor derived from the deformation gradient tensor.

—Compatibility condition:

$$L=\text{grad}\,v=v\otimes\nabla\left(=\frac{\partial v}{\partial x}\right) \tag{25}$$

  where v is the velocity vector and x is the current position vector of the material point X of the soil skeleton, respectively.

- Continuity condition of the soil-water system

$$\left(\int_v dv\right) = \int_v \mathrm{tr}\, D dv = -\int_a v' \cdot n da \tag{26}$$

where v' is the discharge velocity of the pore water and n is the unit outward normal vector at the boundary surface of the soil skeleton, and v and a denote the volume and the area in the current configuration, respectively.

- Darcy's law

$$v' = -k \,\mathrm{grad}\, h = -k\nabla h \left(= -k\frac{\partial h}{\partial x}\right) \tag{27}$$

is the coefficient of permeability.

- Boundary conditions

$$v = \bar{v} \quad \text{on} \quad \Gamma_v, \tag{28}$$

$$\dot{s}_t = \bar{\dot{s}}_t \quad \text{on} \quad \Gamma_{\dot{s}_t} \tag{29}$$

where $\dot{s}_t$ is the nominal stress rate defined in the following manner:

$$\dot{s}_t = \dot{S}_t n \tag{30}$$

$$h = \bar{h} \quad \text{on} \quad \Gamma_h \tag{31}$$

$$v'_n = \bar{v}'_n \quad \text{on} \quad \Gamma_{v'} \tag{32}$$

where v'_n is defined as follows:

$$v'_n = -k\frac{\partial h}{\partial x} \quad \text{on the boundary} \quad \Gamma_{v'}. \tag{33}$$

The weak form of the governing equations, except for Eq. (26), is discretized in space and time for the FEM computation. Equation (26), on the other hand, is computed by the following discretization modified from Akai and Tamura (1978) on the current configuration when the calculation domain is under axi-symmetric condition as seen in Fig. 4 (Asaoka et al., 1994).

$$\int_a \mathrm{tr}\, D da = \sum_{i=1}^{4} \alpha_i (p_i - p), \tag{34}$$

$$\alpha_i = \frac{k}{\rho^f g}\frac{(l_{ri} b_{ri} + l_{zi} b_{zi}) r_i}{l_{ri}^2 + l_{zi}^2}, \tag{35}$$

$$r_i = \frac{r_a + r_b}{2}. \tag{36}$$

Formulations for Dynamic Problems

The dynamic response analysis, based on the finite element method, combined with the multi-dimensional consolidation theory (Biot, 1941) and the elasto-plastic constitutive models, are powerful tools for analyzing the liquefaction of saturated soil during strong earthquakes. Saturated soil is a two-phase material with a skeleton and a pore fluid phase. Biot's equation, governing deformable porous media, can be expressed as

$$\nabla \cdot \sigma + \rho b - \rho \ddot{u} - \rho^f \ddot{w} = 0 \tag{37}$$

where

$$\ddot{w}\left(= \sum_i w_i e_i\right),$$

ρ and ρ^f denote the average relative displacement of pore water, the apparent density of saturated soil and the density of pore water, respectively. If the u-p formulation (Zienkiewicz and Shiomi, 1984), which is popular in recent analyses for dynamic problems, is adopted and assumes that the gradients of porosity and pore water density are smooth enough, the above equation for total mixtures can be simplified as

$$\nabla \cdot \sigma + \rho b - \rho \ddot{u} = 0. \tag{38}$$

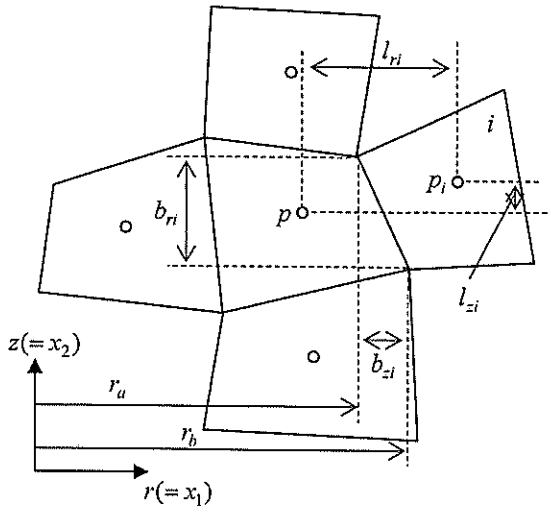

Fig. 4. Computation of the water flow under axi-symmetric condition (after Asaoka et al., 1994)

In the same way, the equilibrium equation for pore water is given as

$$-\nabla p - R^f - \rho^f \ddot{u} + \rho^f b = 0 \tag{39}$$

where p is the pore water pressure. R^f is the body force due to seepage; it is equal to the hydraulic gradient times the unit weight of the pore water. According to Darcy's law, the pore fluid seepage flows through the pores and can be written as

$$\dot{w} = k\frac{R^f}{\rho^f g} \tag{40}$$

where k and g are the permeability tensor and the acceleration of gravity, respectively.

On the other hand, using the principle of effective stress, the continuity equation can be written as

$$\nabla \cdot \dot{w} + \nabla \cdot \dot{u} + \left(\frac{n}{K^f} + \frac{1-n}{K^s}\right)\dot{p} = 0 \tag{41}$$

where K^s, K^f and n are the bulk modulus of the solid material, the bulk modulus of the pore water and the porosity, respectively. From Eqs. (39) to (41), the following equation is obtained:

$$\nabla \cdot \left(\frac{1}{\rho^f g} k \cdot (-\nabla p + \rho^f b)\right) + \nabla \cdot \dot{u} + \left(\frac{n}{K^f} + \frac{1-n}{K^s}\right)\dot{p} = 0. \tag{42}$$

Equations (38) and (42) are coupled to simulate the dynamic behavior of saturated soil as a two-phase material. After the finite element spatial discretization and the Galerkin approximation, the governing equations can be

expressed in the following matrix:

$$M\ddot{U}+\int_{\Omega} B^T\sigma' d\Omega+Qp-f^s=0, \tag{43a}$$

$$Q^T\dot{U}+S\dot{p}+Hp-f^f=0 \tag{43b}$$

where M, U, B, σ', Q, p, S and H are the mass matrix, the displacement vector, the strain-displacement matrix, the effective stress vector determined by the soil constitutive model, the discrete gradient operator coupling the solid and fluid phases, the pore water pressure vector, the compressibility matrix and the permeability matrix, respectively. Vectors f^s and f^f include the effects of the body force and the prescribed boundary conditions for the solid and the fluid phases, respectively. Equations (43a) and (43b) can be integrated in time using a Newmark type of scheme (Newmark, 1959). The solution is obtained for each time step using the modified Newton-Raphson approach.

Shear Strength Reduction Method for Slope Stability Analyses

A shear strength reduction technique for elasto-plastic finite element slope stability analyses has been originally developed by Zienkiewicz et al. (1975). According to the formulations by Ugai (1989), the scheme is summarized below.

At first, the assumed strength parameters, $\tilde{c}$ and $\tilde{\phi}$, replace the corresponding values of c and ϕ in the equation for the failure criterion of the soil. They are defined by dividing c and ϕ by a parameter F, namely,

$$\tilde{c}=\frac{c}{F}, \tag{44a}$$

$$\tan\tilde{\phi}=\frac{\tan\phi}{F}. \tag{44b}$$

Stress and strain are then calculated within the slope based on the conventional elasto-plastic finite element procedure. The initial value of F is assumed to be sufficiently small so as to produce a nearly elastic problem. Then, the value of F is increased, step by step, until a global failure finally develops, when it is judged that the calculations diverge. At this moment, F is considered to be the actual global factor of safety for slope F_s.

Kobayashi et al. (2010) indicated the difference in meanings given for the global factor of safety obtained by the shear strength reduction method and by a rigorous limit analysis with upper and lower bound theorems, from the viewpoint of mathematics and mechanics. They treated this problem as an optimization problem in order to find the minimum value for parameter m, which is a reciprocal of F under the given mechanical conditions. According to a discussion on the concepts of the external plastic work rate and the internal dissipation rate, it has been proved that the relationships between the calculated global factor of safety and the ultimate limit load become nonlinear in the shear strength reduction method if the material is a frictional material. This is different from the limit analysis results in which the relationships are linear. This study provided us with important information to be considered in slope stability analyses based on the elasto-plastic finite element method.

FEM has been used for heat transfer and gas flow, as well as for seepage, and its applications to soil behavior affected by heat conduction or temperature effect can be found. Britto et al. (1992) performed a finite element analysis for the coupled problem of heat flow and consolidation for the disposal of high level radioactive waste buried in the seabed. Savvidou and Britto (1995) carried out a two-dimensional coupled heat conduction and consolidation analysis of soil barriers subjected to temperature gradients. Yashima et al. (1998) analyzed the one-dimensional behavior of natural clay at different strain rates and temperatures. Hibi (2008) developed a dusty gas model for three gas phase components and analyzed the movement of the gas phase components in soil for the design of soil vapor extraction and bio-venting systems, formulating the model by FEM.

In order to simulate soil deformation under difficult conditions, several sophisticated procedures for FEM have been attempted. Poran and Rodriguez (1992) treated the dynamic compaction of dry sand induced by repeated drops of a rigid tamper. They simulated the impact behavior of sand, implementing special computational techniques for the remeshing and the reassignment of the material properties required for large deformation effects and the associated plastic behavior of this type of sand. Asaoka et al. (1998b) proposed a theoretical formulation for the incorporation of constraint conditions imposed upon the displacement/velocity field of the soil-water coupled system along the finite element discretization scheme. The 'no-length change', 'no-angle change' and 'no-direction change' conditions were introduced as internal constraints to the displacement/velocity field via the Lagrange multiplier method.

The formulation of FEM assumes the continuity of variables, which means that great difficulties are faced when simulating phenomena that involve discontinuous variables, such as emanating cracks and propagation whereby the stress and strain become discontinuous. To circumvent these problems, several methods, such as XFEM (e.g., Moes et al., 1999; Budyn et al., 2004) and PDS-FEM (Hori et al., 2005) have been proposed and are presently being developed.

INVERSE ANALYSIS

The success of a numerical simulation, even by means of the highly sophisticated FEM, largely depends on the selection of an appropriate constitutive model and the accuracy of the input data, i.e., the material data for the adopted constitutive model, the initial/boundary conditions, the geometry and so on. The most common way to evaluate the material parameters of the constitutive model incorporated into the FEM is to perform experiments on a soil sample. However, there are shortcomings to these tests: they are twofold. The first is that the deformation fields generated within a soil specimen during the

tests are not necessarily homogeneous. The second is that soil samples are extracted from different soil layers which exhibit a complex heterogenous profile. These shortcomings might lead to a misunderstanding of the identification of the material parameters and to a deterioration in the accuracy of the FEM simulation for the behavior of geotechnical structures.

To reduce the above uncertainties, an inverse method using field measurements during the construction sequence can be adopted to identify uncertain parameters and conditions. Inverse problems are found to be inverted from 'direct' or 'forward' problems, which determine the solution for x under observation y through operator H, based on the equation $y=Hx$. The main objective of inverse methods is to determine uncertain parameters and conditions in a numerical model by comparing measured and numerically computed quantities, i.e., settlement, pore pressure, earth pressure and so on. The numerical strategy for inverse problems is called an 'inverse analysis', and the field of geotechnical engineering has a history of alternatively using a particular term, 'back analysis', in the sense that it is a backward analysis in comparison to a forward analysis.

Inverse problems often encounter threefold ill-posedness whose characteristics are classified as the violation of existence, uniqueness and stability of the solution, namely, the solution for an inverse problem may not exist (the problem is overdetermined), the inverse problem may have many different sets of solutions (the problem is underdetermined) or small changes in input may give rise to large changes in the solution (the location points and the number of required measurements should be chosen properly), even if the corresponding direct or forward problem is well-posed. Several strategies for inverse analyses have been proposed to well-pose these inverse problems. Identification is performed in an iterative way to minimize the following objective function through different manipulations:

$$\min J(x|\beta)=\min\{J_0(x)+\beta J_p(x)\} \tag{45}$$

where

$$J_0(x)=\{y^{obs}-y(x)\}^T R^{-1}\{y^{obs}-y(x)\},$$
$$J_p(x)=(x-\bar{x})^T M^{-1}(x-\bar{x})$$

and β is a positive scalar adjusting the relative significance of the observation to prior information. A set of values for β and R branches into the following subclasses of inverse analyses:

1) Least squares method ($\beta=0$, $R=I$)
   This method was the most common tool in earlier works for inverse analyses in geotechnical engineering. The technique provides a numerical solution for overdetermined inverse problems, but cannot give any unique solution for underdetermined problems.
2) Maximum likelihood method ($\beta=1$, $R\neq I$)
   The difference between the least squares method and this technique is the weight of each observation, depending on its significance. The resultant objective function of the projection filter (Tosaka and Utani, 1993) eventually coincides with this function.
3) Bayesian method/Kalman or Extended Kalman filter ($\beta=1$, $R\neq I$)
   A formulation manipulated from a statistical viewpoint provides this type of objective function and relates to Tikhonov's regularization (Tikhonov, 1963) when $\bar{x}=0$. The extended Kalman filter can deal with the nonlinear state/observation equations by linearization with a Taylor series expansion.
4) Extended Bayesian method (β: optimal, $R\neq I$)
   A scalar parameter, β, relatively adjusts the significance between observation and prior information by considering the AIC (Akaike Information Criterion; Akaike, 1978); the ABIC (Akaike-Bayesian Information Criterion; Honjo and Kashiwagi, 1991).
5) Data assimilation by Ensemble Kalman filter/Particle filter
   Data assimilation is an innovative tool which extends the inverse analysis to combine observations of the current state of a system with results from a mathematical model to produce an analysis, providing the best estimate of the current state of the system. The ensemble of the Kalman filter (EnKF; Evensen, 1994) and the particle filter (PF; Kitagawa, 1996; Gordon et al., 1993) has been developed for sequential data assimilation instead of the Kalman/extended Kalman filter applied in earlier works, namely, until the middle of the 1990s. In both filters, the predictive probability density functions of state variables are constructed by ensembles or particles obtained from the Monte Carlo simulation. Both filters can be easily applied to strong nonlinear problems, such as soil-water coupled problems, based on elasto-plastic geomaterials. The filters are also applicable to non-Gaussian distributions of parameters. As the ensemble size or the number of particles increases, the EnKF or the PF should converge to the exact Kalman filter.

Inverse analysis techniques have been applied to geotechnical problems since the 1980s (Asaoka, 1978; Asaoka and Matsuo, 1982, 1984). Their use makes it easier to evaluate the performance of geotechnical structures such as the settlement prediction of embankment foundations (Arai et al., 1984; Shoji et al., 1990; Ichikawa, et al., 1992; Nishimura et al., 2002, 2005), the observation construction control system for embankments (Shoji et al., 1989), the investigation of the seismic properties of soil (Arai et al., 1990; Honjo et al., 1998) and pile-soil interaction by neural networks (Nagaoka et al., 2001) and by ABIC (Honjo et al., 2005) etc., by a quantifiable observational method. Recently, Murakami et al. have dealt with data assimilation in geotechnical engineering by applying the particle filter to the settlement behavior at Kobe Airport, constructed on reclaimed land, to identify a set of parameters in an elasto-plastic constitutive model (Murakami et al., 2009; Shuku et al., 2010).

MESH-FREE METHODS, SPH, FINITE VOLUME METHOD AND SO ON

Mesh-free methods have recently appeared as connectivity-free between elements and nodes as alternatives to FEM, which suffers from a high incidence of numerical errors caused by distorted or low quality meshes (Nguyen et al., 2008; Liu, 2009). In addition, due to the underlying structure of mesh-based methods, it is difficult to deal with discontinuities which do not align with element edges. The remedies for such limitations are remeshing and discontinuous enrichment; however, the former is time-consuming and requires much human labor and the latter can be achieved only through particular types of elements within the context of FEM. Mesh-free methods, on the other hand, have some advantages in overcoming the above difficulties. Table 1 lists some mesh-free methods that have been developed so far.

The first attempt to apply mesh-free methods to geotechnical problems was made by Modaressi and Aubert (1998) using EFG with an elastic constitutive model. This was extended by Murakami et al. (2005) using an elastoplastic constitutive model within a finite deformation. Karim et al. (2002) applied this technique to the analysis of a transient response of elastic saturated soil on the seabed under cyclic loading due to wave motion. Sato and Matsumaru (2006) used the EFG method to analyze liquefaction phenomena when it became impossible to continue the computation within a large deformation regime with the usual FEM. Oliaei et al. (2008) developed a new formulation of EFG for solving coupled hydro-mechanical problems, and Kumar and Dodagoudar (2009) made an attempt to provide a simple, but sufficiently accurate methodology for the numerical simulation of the two-dimensional contaminant transport through saturated homogeneous porous media and landfill liners using EFG to overcome some difficulties when dealing with advection-dominant transport problems by conventional mesh-based numerical methods which depend on mesh/grid size and element connectivity.

Meshless strategies, except for EFG, have been applied to geotechnical problems. Wang et al. (2001) used PIM to solve Biot's consolidation equation for elastic materials, Nogami et al. (2004) incorporated the double porosity model into the radial PIM to analyze lumpy clay fillings, and Wu et al. (2001) introduced a Lagrangian reproducing kernel formulation into the analysis for clay stratum subjected to footing load.

Smoothed Particle Hydrodynamics (SPH) is also within the category of mesh-free methods used to approximate the strong form of a partial differential equation (PDE) by choosing a smooth kernel and using it to localize the strong form of the PDE through a convoluted integration (Gingold and Managhan, 1977; Lucy, 1977). So far, many improvements have been incorporated to overcome the instabilities and inconsistencies in numerical computations, *see*, e.g., Li and Liu (2002), Liu and Liu (2010).

With regard to geotechnical applications of the SPH, Maeda et al. have applied this technique to the generation of air bubbles within a soil and to seepage failure in the context of soil-liquid-gas interaction (Maeda et al., 2006, 2010). Bui et al. (2008) implemented the Drucker-Prager model with the associated/non-associated flow rule into the SPH to allow the solving of elastic-plastic flows of soil, and applied the proposed strategy to a large deformation and the post-failure of cohesive/non-cohesive soil (Bui et al., 2008). Li et al. (2007) have developed a coupled discrete particle-continuum model for saturated granular materials, characteristic-based Smoothed Particle Hydrodynamics (CBSPH) which models pore fluid flows relative to the deformed solid phase as a packed assemblage of interacting discrete particles with voids by DEM (Li et al., 2007).

The finite volume method (FVM) has been a powerful tool for numerically solving partial differential equations, especially for fluid dynamics, such as the Navier-Stokes equations and shallow water equations, and recent developments in the method are remarkable. The *Journal of Computational Physics* is one of the most helpful journals in giving an overview of the method, because it includes a large number of papers related to the fundamentals and applications of FVM. The method divides a computational domain into a sufficient number of cells, which are analogous to elements for FEM. FEM gives the calculated values at the nodal points, while FVM outputs them at the centroids of the cells. FVM realizes a low computational load and is advantageous in that it can stably solve differential equations with advective terms. As for computational studies on geotechnical problems, Nishigaki et al. (1986) applied FVM to a saturated-unsaturated seepage analysis, although they described the method as

Table 1. Overview of some mesh-free methods (revised from Liu, 2009)

Method	References	Formulation procedure	Local function approximation
Diffuse element method	Nayroles *et al.*	Galerkin weak form	MLS
EFG or EFGM	Belytshcko *et al.*	Galerkin weak Form	MLS
MLPG	Atluri *et al.*	Local Petrov-Galerkin	MLS
PIMs	Liu *et al.*	Local Petrov-Galerkin	Point interpolation using polynomial and radial basis fn.
SPH	Lucy; Gingold and Monaghan	Strong form	Integral representation, Particle approximation
GSM	Liu *et al.*	Weakform-like	Point interpolation
Finite point method	Onate *et al.*	Strong form	MLS
RKPM	Liu *et al.*	Strong or weak form	Reproducing kernel
hp-Clouds	Oden and Abani	Strong or weak form	Partition of unity, MLS
Partition of unity FEM	Babuska and Melenk	Weak form	Partition of unity, MLS

an 'Integrated Finite Difference Method (IFDM)', and Fujisawa et al. (2010) have used the method to solve the advection equation of eroded soil particles migrating within soils. Rapid advancements are being made with FVM and its potential for use in geotechnical applications is expected to be soon realized.

DYNAMICS

Strictly speaking, all phenomena should be regarded as dynamic problems. However, if the deformation of an object is slow enough, from an engineering point of view, it can be said that the behavior is affected by neither velocity nor acceleration. A strategy of formulations well known as a 'static' analysis, which ignores the viscous resistance and the inertial force, is widely used for such problems.

On the other hand, high-speed deformation phenomena with wave propagations, induced by seismic motion and impact force, etc., are usually modeled as 'dynamic' problems. In these sorts of problems, the behavior can be generally described with the equation of motion of the system. This equation is often represented as the following simple equation, which was originally extended from the concept of the Voigt model for a conventional single-degree-of-freedom model with mass, spring and dashpot.

$$M\ddot{U}+C\dot{U}+KU=f \tag{46}$$

where M, C and K are the mass, viscosity and stiffness matrices for the discretized system, respectively. U and f are the relative displacement vector to the fixed base in the analysis and the external force vector acted to the system, respectively. In usual seismic response analyses, f is given as the inertia force induced by the input base motion. This model is used most frequently nowadays, because its performance has been proved to be quite similar to the real dynamic behavior of soil and structures, according to the results of many demonstrative studies on various objects.

Generally speaking, numerical methods applied to solve the above equation directly are called 'dynamic response analyses', and they are classified into two kinds of analyses, i.e., analyses in the frequency domain and analyses in the time domain.

The former, analyses in the frequency domain, are often used for assessing the vibration mode and the eigenvalues of the system (e.g., Kagawa, 1983; Sakaki et al., 1985; Pitilakis and Moutsakis, 1989; Watanabe and Kawakami, 1995). Here, the analyzed system is usually assumed to behave as a linear material, including the equivalent linear modeling. This simplification is due to the limitation of mathematical procedures like the Fourier transform. Since the response is assumed to be linear, the residual deformation that remains after an earthquake cannot of course be predicted directly by this type of analysis.

The latter, analyses in the time domain, comprise a more popular strategy for simulating the actual phenomena precisely. They directly integrate the equation of motion and are based on a time integration scheme such as the Newmark's β method. It is easy to take into account the material nonlinearity, including changes in soil properties with time. In early times, this type of analysis was applied mainly for seismic response analyses of 1D multi-layered grounds (Oka et al., 1981; Kawamoto et al., 1982), which are rather simple problems.

Before long, the progress of computer technology after the 1990s brought about the rapid increase in the capacity of computer memory and the speed of computing. Many complicated problems, thought to be impossible to remedy in the past, were solved after the use of powerful computers. As an example, a skillful method to predict the residual deformation of an embankment after an earthquake, by combining an equivalent linear dynamic analysis and an elasto-plastic static analysis, was reported by Kuwano et al. (1991). Of course, the development of the numerical analysis was accomplished by the improvement of the numerical technique as well as by the computer itself. Fundamental studies on the essential elements in numerical procedures have also been conducted by many researchers, e.g., lateral dashpots in BEM by Fukuwa and Nakai (1989), the modification of input motion by Hunaidi et al. (1990), infinite boundaries by Anandarajah (1993), the large deformation effect by Li and Ugai (1998), the limitations of the coupled dynamic analysis by Pietruszczak and Parvini (2001) and nonlinear amplification by Tokimatsu and Sekiguchi (2006).

It is known that among the most common problems in geotechnical earthquake engineering are the problems related to earth structures. Many finite element studies on earth structures mainly focused on the prediction of residual deformation, using the elasto-plastic models in total stress formulations (e.g.,Psarropoulos et al., 2007; Feizi-Khankandi et al., 2009; Wakai et al., 2010), which are sufficiently simple and convenient for engineering practice in seismic design. The shakedown analysis was also tried, and was one of the more skillful techniques in design practice (Ohtsuka et al., 1998).

As a more rigorous way of modeling, constitutive models in effective stress formulations can be applied to the soil-water coupled problems. Finite element codes equipped with such numerical models can simulate a so-called liquefaction phenomenon, or strain softening under cyclic loading, due to the increase in and the dissipation of the excess pore water pressure in a saturated ground during and after a strong earthquake (e.g., Matsuo et al., 2000; Onoue et al., 2006; Namikawa et al., 2007), which is one of the most important design issues to be resolved nowadays. Various constitutive models have been introduced into the finite element analysis with the appropriate nonlinear algorithms, encouraged by the progress of the modeling of soil properties described in elasto-plastic frameworks. Among the most essential and impressive research in the field of numerical analysis recently is the work Noda et al. (2008) have done in developing a new numerical model based on the soil skeleton-pore water coupled equation that includes the effect of the

inertia term. This method allows changes in the geometric shape of the soil to be taken into account and is capable of dealing with all types of external forces irrespective of whether they are static or dynamic.

The purpose of dynamic response analyses for earth structures is mainly to predict the residual deformation of the embankment and the ground precisely, which accords with the requirements in design practice improved after the Kobe earthquake. The most important concern in seismic design is the gradual switching over from the "ultimate state" to the "allowable deformation" of each structure. Such a point of view will be helpful in developing a performance-based design code in the near future.

Many finite element studies on the ground-structure system subjected to earthquake motion have been conducted as well, e.g., bridge and pile foundations by Kimura and Zhang (2000) and Zhang and Kimura (2002), the simulation of statnamic load tests by Kimura and Boonyatee (2002), quay walls and seawalls by Iai and Kameoka (1993), Kanatani et al. (2001) and Dakoulas and Gazetas (2005) and tunnels by Khoshnoudian and Shahrour (2002). It is very important for such ground-structure problems to improve the modeling of the dynamic and nonlinear interaction between the ground and the structures.

SLOPE STABILITY

An evaluation of slope stability is always required for the design of embankments and slope cutting, which are well known as typical engineering problems in geotechnical engineering. In engineering practice, it has been recognized that the stability of slopes can be evaluated by an engineering concept based on the global factor of safety for slope failure, where the balance of the sliding force due to the self weight and the shear resistance of the soil in the slope are considered. This concept can also include a pseudo-static seismic force component used in conventional seismic design. In this sort of method, the soil is assumed to be a rigid perfectly-plastic material with no elastic deformation. Such a simplification makes it possible to realize simple numerical methods for slope stability analyses which are useful for design practice. It is also important that such a design strategy be regarded as an engineering decision on the safer side.

One of the most popular slope stability analysis methods is the limit equilibrium method (e.g., Jiang and Yamagami, 2004; Cheng and Zhu, 2004; Zheng et al., 2009). It is applied to evaluate the global factor of safety based on the comparison of forces acting along the assumed slip surface of a slope, i.e., the sliding force due to the self weight and the maximum shear resistance of the soil. In practice, for convenience, the forces are often evaluated for each slice into which the sliding block is divided. One of the key issues in this method is the use of appropriate shear strength parameters mobilized along the assumed slip surface (e.g., Shogaki and Kumagai, 2008).

Although this method is easy to use and has been widely applied to engineering practice, it may often provide imperfect solutions, because the internal forces in the sliding block cannot be considered appropriately with this method. A more reliable method within rigid perfectly-plastic frameworks may be the limit analysis method, which is rigorously based on appropriate limit mechanical theorems (e.g., Baker, 2004). This method can provide perfect solutions for the ultimate state of the slope, where all the required mechanical conditions are taken into account in its formulations.

The global factor of safety can also be evaluated by the elasto-plastic finite element analysis with the shear strength reduction method (SSRM) (Ugai, 1989; Matsui, 1992), which was originally proposed by Zienkiewicz et al. (1975). The elasto-plastic FEM was also applied to reinforced slope problems (Matsui and San, 1989, 1990; Kodata et al., 1995; Zornberg and Kavazanjian, 2001) and problems with stabilizing piles in a slope (Cai and Ugai, 2000). Slope failures induced by heavy rainfall can be evaluated by the combination of the seepage analysis and the stability analysis (Toyota et al., 2006; Wei and Cheng, 2010). If the soil is assumed to be a strain-softening material in the analysis, a progressive failure of the slope can be simulated by an elasto-plastic FEM (Zhang et al., 2003; Ye et al., 2005), which is useful for simulating the process of slope failure precisely. The global factor of safety obtained from FEM with SSRM was compared to the one from the limit equilibrium method (San et al., 1994; Ugai and Leshchinsky, 1995), showing that these factors are mostly close to each other. Strictly speaking, it has been indicated that the physical meaning of the global factor of safety evaluated by FEM with SSRM is slightly different from the meaning by the aforementioned limit analysis (Kobayashi et al., 2010). This may cause a problem in cases where the factor should be treated as a physical value with quantitative meanings.

The concept of the ultimate state corresponding to the slope failure with a clear slip surface is very convenient for engineering purposes. However, the actual phenomena do not always agree with such a mechanism, especially in cases where the seismic motion causes the slope to be deformed largely without collapse. Therefore, for the evaluation of slope stability at the time of a strong earthquake, the focus of the analysis is often placed on the residual deformation, not on the global factor of safety. Such a deformation can be easily predicted by the dynamic response analysis based on the elasto-plastic finite element method (e.g., Li and Ugai, 1998; Wakai and Ugai, 2004; Onoue et al., 2006). One of the essential items in such simulations is to consider the soil properties under cyclic loading appropriately, for example, the strain amplitude dependency in the apparent shear modulus and the damping ratio. In addition, if the soil is assumed to be a strain-softening material under cyclic loading, a long distance travelling failure of the slope can be simulated numerically (Wakai et al., 2010), which has sometimes been observed at the time of recent strong earthquakes.

Furthermore, as a conventional method of prediction, Newmark's sliding block theory (Newmark, 1965), which

uses the critical seismic coefficient obtained from the limit equilibrium slope stability analysis, can be used to predict the sliding displacement during an earthquake (e.g., Shinoda et al., 2006). This method is very simple and useful for design, but users should understand the limitations of the coverage of its application field due to the incompleteness in the mechanical assumptions used in the method.

EMBANKMENT/EXCAVATION

Embankments, such as earth-fill dams, levees and road embankments, are the most common earth structures and have been important targets for soil mechanics. The settlement of the ground due to embankment loading and the stability of the embankments have been of such great interest in practice that a number of computational studies have been done to predict the behavior of the embankments using several numerical methods. Among the methods, FEM has been a central method up to now. The estimation of deformation and stability requires the determination of the stress state within the earth structures by solving the equilibrium equation for static problems or the momentum equation for dynamic problems with relevant constitutive models. Adopting the concept of effective stress involves the simultaneous analysis of water seepage with the stress state to determine the distribution of pore water pressure, which leads to the so-called soil-water coupled analysis. For a seepage analysis of embankments subjected to ceaseless or frequent water seepage, the technique proposed by Neumann (1973), giving the natural boundary condition at the seepage faces, has often been employed.

Finite element analyses of embankment deformation appeared in the 1970s. Shoji and Matsumoto (1976) applied FEM and conducted soil-water coupled analyses, assuming a small deformation, to calculate the consolidation of embankment foundations. Narita and Ohne (1978) investigated the cracking potential caused by differential settlements in the longitudinal sections of high embankments by a numerical simulation with FEM. These early computational works regarded the embankments as (linearly) elastic materials and were oriented toward static problems. Elastic deformation analyses can predict the deformation of structures, but entail difficulties in predicting the slip surfaces or sliding.

Dynamic analyses of soil structures are realized by directly solving the equation of motion with a time integration scheme as well as by spatial discretization methods such as FEM. Taniguchi et al. (1983) numerically calculated the final displacement of earth dams induced by an earthquake, conducting an equivalent static analysis with FEM. Kuwano et al. (1991) carried out both a nonlinear static analysis and an equivalent linear dynamic analysis to estimate the residual deformation of embankments after earthquakes.

As the nonlinear computation scheme and the constitutive models for soil, treating the developed elasto-plasticity or elasto-viscoplasticity, the finite element analysis innovating these models became popular for the prediction of the deformation and the stability of embankments in both static and dynamic problems (e.g., Iizuka and Ohta, 1987; Sakajo and Kamei, 1996; Matsuo et al., 2000; Iizuka et al., 2003; Pagano et al., 2009). The above finite element analysis with these models has been utilized for the recent performance-based design of earth dams (e.g., Tani et al., 2009; Sica and Pagano, 2009). Elasto-plastic and elasto-viscoplastic models require the current stress to calculate the relation of the stress and strain rate. When these models are applied to predict the mechanical behavior of an embankment, it should be noted that the initial stress distribution within the embankment is necessary and that the construction analysis is a feasible process for obtaining the initial stress state. Recently, the combination of a rate-based elasto-plastic constitutive model and the FEM of the finite deformation formulation has enabled the continuous analysis of the construction, the consolidation, the earthquake response, the deformation and the stability of embankments after earthquakes (Noda et al., 2009).

Excavation, such as tunneling, is an unloading procedure, contrary to the construction of embankments. The finite element analysis of an excavation requires the release of the equivalent nodal forces of the earth pressure of the excavated elements and the removal of their stiffness, while the construction analysis of embankments involves the application of the equivalent nodal weight of the constructed elements and the generation of their stiffness. The basic procedure for the release of earth pressure is summarized as follows:

1. Calculate the equivalent nodal forces of the earth pressure of the excavated elements.
2. Apply the nodal forces equal in magnitude and opposite in sign to the excavation surface.

Several numerical analyses of excavations have been done by Christian and Wong (1973), Nakai et al. (1997), Komiya et al. (1999) and Nakai et al. (2007), for instance. A detailed review concerning excavation is presented in the paper entitled 'Model Test and Numerical Analysis Methods in Tunnel Excavation Problem' in this issue.

SHEAR BAND FORMATION AND LOCALIZATION

FEM has been applied to a variety of geotechnical problems, such as shear band formulation, progressive failure, bifurcation, gas flow, parameter identification, as well as soil deformation and seepage. A number of works have been devoted to the numerical simulation of consolidation, the shearing behavior, and seepage (e.g., Kono, 1974; Matsumoto, 1976; Matsui and Abe, 1981; Matsuoka et al., 1990; Maekawa et al., 1991; Hsi and Small, 1993; Yashima et al., 1998; Asaoka et al., 1998a; Conte, 1998).

The implementation of the finite deformation theory into finite element analyses permitted the tracking of the soil deformation close to failure, which enabled shear-band formulation and bifurcation to be numerically simulated by FEM. Yatomi et al. (1989) conducted a soil-

water coupled analysis with FEM and succeeded in simulating the formulation of shear bands with a non-coaxial Cam-clay model by formulating finite strain and employing the updated Lagrangean scheme. Tanaka and Sakai (1993) analyzed the progressive failure and the scale effect of trap-door problems, developing an elasto-plastic model including the shear band effect. Asaoka and Noda (1995) simulated imperfection-sensitive bifurcation by a soil-water coupled finite deformation analysis. They revealed that one of the possible reasons for the rate dependency of the undrained shear strength of saturated clay was the effect of pore water migration on the imperfection-sensitive bifurcation behavior of saturated clay. Strain localization into shear bands was taken into consideration for the numerical simulation of the bearing capacity characteristics of strip footing on sand (Siddiquee et al., 1999). An elasto-viscoplastic constitutive model was extended to describe the instability of the failure state which is connected to structural degradation. The model can reproduce the apparent compressive strain localization regarded as compaction bands, when structural degradation is considered (Kimoto and Oka, 2005).

SUMMARY

In this survey, numerical methods and their applications developed over several decades in geotechnical engineering have been reviewed. In this overview, most of references are among papers appeared in Soils and Foundations except specific papers from other journals dealing with related topics. Simulation methods developed over fifty years are classified into six categories according to the methodologies as the 'warp' of this review, and their details and characteristics are presented except two categories, namely, 'Limit theorems' and 'Micromechanics and DEM', because they are summarized in other chapters within this special issue. Applications of such simulation methods are also classified into five categories as the 'woof' of this review based on subject matters related to phenomena to facilitate type of order to this survey. Although the advances in computational methods for geomechanics have reached the same level of or almost surpassed those of other engineering fields in the past decades, there still many tasks and challenges remaining to solve the complex behavior of soils.

REFERENCES

1) Akai, K. and Tamura, T. (1978): Numerical analysis of multi-dimensional consolidation accompanied with elasto-plastic constitutive equation, *Proc. JSCE*, (269), 95–104 (in Japanese).
2) Akaike, H. (1978): A new look at Bayes procedure, *Biometrika*, 65, 53–59.
3) Anandarajah, A. (1993): Dynamic analysis of axially-loaded footings in time domain, *Soils and Foundations*, 33(1), 40–54.
4) Arai, K., Ohta, H. and Kojima, K. (1984): Estimation of soil parameters based on monitored movement of subsoil under consolidation, *Soils and Foundations*, 24(4), 95–108.
5) Arai, K., Iida, K. and Konja, A. (1990): A simple back-analysis in a seismic subsoil context, *Soils and Foundations*, 30(4), 175–182.
6) Arai, K. (1993): Back-analysis of deformation and Mohr-Coulomb strength parameters based on initial strain method, *Soils and Foundations*, 33(3), 130–138.
7) Asaoka, A. (1978): Observational procedure of settlement prediction, *Soils and Foundations*, 18(4), 87–101.
8) Asaoka, A. and Matsuo, M. (1982): An inverse problem approach to settlement prediction, *Soils and Foundations*, 20(4), 53–65.
9) Asaoka, A. and Matsuo, M. (1984): An inverse problem approach to the prediction of multi-dimensional consolidation behavior, *Soils and Foundations*, 24(1), 49–62.
10) Asaoka, A., Nakano, M. and Noda, T. (1994): Soil-water coupled behavior of saturated clay near/at ciritical state, *Soils and Foundations*, 34(1), 91–105.
11) Asaoka, A. and Noda, T. (1995): Imperfection-sensitive bifurcation of Cam-clay under plane strain compression with undrained boundaries, *Soils and Foundations*, 35(1), 83–100.
12) Asaoka, A., Nakano, M. and Noda, T. (1997): Soil-water coupled behavior of heavily overconsolidated clay near/at critical state, *Soils and Foundations*, 37(1), 13–28.
13) Asaoka, A., Noda, T. and Fernando, G. S. K. (1998a): Consolidation deformation behavior of lightly and heavily overconsolidated clay foundations, *Soils and Foundations*, 38(2), 75–91.
14) Asaoka, A., Noda, T. and Kaneda, K. (1998b): Displacement/traction boundary conditions represented by constraint conditions on velocity field of soil, *Soils and Foundations*, 38(4), 173–181.
15) Baker, R. (2004): Stability chart for zero tensile strength materials with a non-linear failure criterion-variational solution and its engineering implications, *Soils and Foundations*, 44(3), 125–132.
16) Biot, M. (1941): General theory of three dimensional consolidation, *Journal of Applied Physics*, 12, 155–164.
17) Britto, A. M., Savvidou, C., Gunn, M. J. and Booker, J. R. (1992): Finite element analysis of the coupled heat flow and consolidation around hot buried objects, *Soils and Foundations*, 32(1), 13–25.
18) Budyn, E., Zi, G., Moes, N. and Belytschko, T. (2004): A method for multiple crack growth in brittle materials without remeshing, *Int. J. Numer. Methods Eng.*, 61, 1741–1770.
19) Bui, H. H., Fukagawa, R., Sako, K. and Ohno, S. (2008): Lagrangian meshfree particles method (SPH) for large deformation and failure flows of geomaterial using elastic-plastic soil constitutive model, *Int. J. Numer. Anal. Meth. Geomech.*, 32, 1537–1570.
20) Cai, F. and Ugai, K. (2000): Numerical analysis of the stability of a slope reinforced with piles, *Soils and Foundations*, 40(1), 73–84.
21) Cheng, Y. M. and Zhu, L. J. (2004): Unified formulation for two dimensional slope stability analysis and limitations in factor of safety determination, *Soils and Foundations*, 44(6), 121–127.
22) Christian, J. T. and Wong, I. H. (1973): Errors in simulating excavation in elastic media by finite elements, *Soils and Foundations*, 13(1), 1–10.
23) Conte, E. (1998): Consolidation of anisotropic soil deposits, *Soils and Foundations*, 38(4), 227–237.
24) Dakoulas, P. and Gazetas, G. (2005): Seismic effective-stress analysis of caisson quay walls: Application to Kobe, *Soils and Foundations*, 45(4), 133–148.
25) Evensen, G. (1994): Sequential data assimilation with a non-linear quasi-geostrophic model using Monte Carlo methods to forecast error statistics, *Journal of Geophysical Research*, 99(C5), 10143–10162.
26) Feizi-Khankandi, S., Ghalandarzadeh, A., Mirghasemi, A. A. and Hoeg, K. (2009): Seismic analysis of the garmrood embankment dam with asphaltic concrete core, *Soils and Foundations*, 49(2), 153–166.
27) Fujisawa, K., Murakami, A. and Nishimura, S. (2010): Numerical analysis of the erosion and the transport of fine particles within soils leading to the piping phenomenon, *Soils and Foundations*, 50(4), 471–482.
28) Fukuwa, N. and Nakai, S. (1989): A study on lateral dashpots for soil-structure interaction and its application to a simplified technique, *Soils and Foundations*, 29(3), 25–40.
29) Gingold, R. A. and Monaghan, J. J. (1977): Smoothed particle

hydrodynamics: theory and application to non-spherical stars, *Monthly Notices R. Astron. Soc.*, **181**, 375–389.
30) Gordon, N. J., Salmond, D. J. and Smith, A. F. M. (1993): Novel approach to nonlinear/non-Gaussian Bayesian state estimation, *IEE Proc. F*, **140**(2), 107–113.
31) Hibi, Y. (2008): Formulation of a dusty gas model for multi-component diffusion in the gas phase of soil, *Soils and Foundations*, **48**(3), 419–432.
32) Honjo, Y. and Kashiwagi, N. (1991): On the optimum design of a smoothing filter for geophysical tomography, *Soils and Foundations*, **31**(1), 131–144.
33) Honjo, Y., Iwamoto, S., Sugimoto, M., Onimaru, S. and Yoshizawa, M. (1998): Inverse analysis of dynamic soil properties based on seismometer array records using the extended Bayesian method, *Soils and Foundations*, **38**(1), 131–143.
34) Honjo, Y., Zaika, Y. and Pokharel, G. (2005): Estimation of subgrade reaction coefficient for horizontally loaded piles by statistical analyses, *Soils and Foundations*, **45**(3), 51–70.
35) Hori, M., Oguni, K. and Sakaguchi, H. (2005): Proposal of FEM implemented with particle discretization for analysis of failure phenomena, *Journal of the Mechanics and Physics of Solids*, **53**(3), 681–703.
36) Hsi, J. P. and Small, J. C. (1993): Application of a fully coupled method to the analysis of an excavation, *Soils and Foundations*, **33**(4), 36–48.
37) Hunaidi, M. O., Towhata, I. and Ishihara, K. (1990): Modification of seismic input for fully discretized models, *Soils and Foundations*, **30**(2), 114–118.
38) Iai, S. and Kameoka, T. (1993): Finite element analysis of earthquake induced damage to anchored sheet pile quay walls, *Soils and Foundations*, **33**(1), 71–91.
39) Ichikawa, Y. and Ohkami, T. (1992): A parameter identification procedure as a dual boundary control problem for linear elastic materials, *Soils and Foundations*, **32**(2), 35–44.
40) Iizuka, A. and Ohta, H. (1987): A determination procedure of input parameters in elastic-plastic finite element analysis, *Soils and Foundations*, **27**(3), 71–87.
41) Iizuka, A., Yamamoto, N., Sueoka, M., Sato, N., Kawaida, M. and Ohta, H. (2003): Derformation analysis of soft subsoil on sloping bedrock loaded by highway embankment with stabilization methods, *Soils and Foundations*, **43**(5), 81–92.
42) Jiang, J. C. and Yamagami, T. (2004): Three-dimensional slope stability analysis using an extended Spencer method, *Soils and Foundations*, **44**(4), 127–136.
43) Kagawa, T. (1983): Lateral pile-group response under seismic loading, *Soils and Foundations*, **23**(4), 75–86.
44) Kanatani, M., Kawai, T. and Tochigi, H. (2001): Prediction method on deformation behavior of caisson-type seawalls covered with armored embankment of man-made islands during earthquakes, *Soils and Foundations*, **41**(6), 79–96.
45) Karim, M. R., Nogami, T. and Wang, J.-G. (2002): Analysis of transient response of saturated porous elastic soil under cyclic loading using element-free Galerkin method, *Int. J. Solids and Structures*, **39**, 6011–6033.
46) Kawamoto, T., Ichikawa, Y. and Togashi, Y. (1982): Effects of nonlinearity of soil foundations in dynamic analysis, *Soils and Foundations*, **22**(4), 152–160 (in Japanese).
47) Khoshnoudian, F. and Shahrour, I. (2002): Numerical analysis of the seismic behavior of tunnels constructed in liquefiable soils, *Soils and Foundations*, **42**(6), 1–8.
48) Kimoto, S. and Oka, F. (2005): An elasto-viscoplastic model for clay considering destructuralization and consolidation analysis of unstable behavior, *Soils and Foundations*, **45**(2), 29–42.
49) Kimura, M. and Zhang, F. (2000): Seismic evaluations of pile foundations with three different methods based on three-dimensional elasto-plastic finite element analysis, *Soils and Foundations*, **40**(5), 113–132.
50) Kimura, M. and Boonyatee, T. (2002): Statnamic load tests on model piles and their 3D-elastoplastic FEM analysis, *Soils and Foundations*, **42**(1), 71–87.
51) Kitagawa, G. (1996): Monte Carlo filter and smoother for non-Gaussian nonlinear state space model, *Journal of Computational and Graphical Statistics*, **5**(1), 1–25.
52) Kobayashi, S., Nishiki, Y., Shimominami, T. and Matsumoto, T. (2010): A study on shear strength reduction method from the point of mathematics and mechanics, *Jour. of Applied Mechanics*, JSCE, **13**, 401–409 (in Japanese).
53) Kodaka, T., Asaoka, A. and Pokharel, G. (1995): Model tests and theoretical analysis of reinforced soil slopes with facing panels, *Soils and Foundations*, **35**(1), 133–145.
54) Komiya, K., Soga, K., Akagi, H., Hagiwara, T. and Bolton, M. D. (1999): Finite element modelling of excavation and advancement processes of a shield tunnelling machine, *Soils and Foundations*, **39**(3), 37–52.
55) Kono, I. (1974): Finite element analysis of a nonsteady seepage problem, *Soils and Foundations*, **14**(4), 75–85.
56) Kumar, R. P. and Dodagoudar, G. R. (2009): Modelling of contaminant transport through landfill liners using EFGM, *Int. J. Numer. Anal. Meth. Geomech.*, **34**(7), 661–688.
57) Kuwano, J., Ishihara, K., Haya, H. and Izu, F. (1991): Analysis on permanent deformation of embankments caused by earthquakes, *Soils and Foundations*, **31**(3), 97–110.
58) Li, Q. and Ugai, K. (1998): Comparative study on static and dynamic sliding behaviors of slopes based on small and large deformation theories, *Soils and Foundations*, **38**(3), 201–207.
59) Li, S. and Liu, W. K. (2002): Meshfree and particle methods and their applications, *Appl. Mech. Rev.*, **55**(1), 1–34.
60) Li, X., Chu, X. and Sheng, D. C. (2007): A saturated discrete particle model and characteristic-based SPH method in granular materials, *Int. J. Numer. Methods Eng.*, **72**, 858–882.
61) Liu, G. R. (2009): *Meshfree Methods-Moving Beyond the Finite Element Method*, CRC Press.
62) Liu, M. B. and Liu, G. R. (2010): Smoothed particle hydrodynamics (SPH): an overview and recent developments, *Arch. Comput. Methods Eng.*, **17**, 25–76.
63) Lucy, L. B. (1977): A numerical approach to the testing of the fission hypothesis, *Astron. J.*, **82**, 1013–1024.
64) Maeda, K., Sakai, H. and Sakai, M. (2006): Development of seepage failure analysis method of ground with Smoothed Particle Hydrodynamics, *Structural Eng./Earthquake Eng.*, **23**(2), 307–319.
65) Maeda, K. and Sakai, H. (2010): Seepage failure and erosion of ground with air bubble dynamics, *Geoenvironmental Engineering and Geotechnics* (GSP 204), ASCE, 261–266.
66) Maekawa, H., Miyakita, K. and Sekiguchi, H. (1991): Elasto-viscoplastic consolidation of a diatomaceous mudstone, *Soils and Foundations*, **31**(2), 93–107.
67) Matsui, T. and Abe, N. (1981): Multi-dimensional elasto-plastic consolidation analysis by finite element method, *Soils and Foundations*, **21**(1), 79–95.
68) Matsui, T. and San, K. C. (1989): An elastoplastic joint element with its application to reinforced slope cutting, *Soils and Foundations*, **29**(3), 95–104.
69) Matsui, T. and San, K. C. (1990): A hybrid slope stability analysis method with its application to reinforced slope cutting, *Soils and Foundations*, **30**(2), 79–88.
70) Matsui, T. and San, K. C. (1992): Finite element slope stability analysis by shear strength reduction technique, *Soils and Foundations*, **32**(1), 59–70.
71) Matsumoto, T. (1976): Finite element analysis of immediate and consolidation deformations based on effective stress principle, *Soils and Foundations*, **16**(4), 23–34.
72) Matsuo, O., Shimazu, T., Uzuoka, R., Mihara, M. and Nishi, K. (2000): Numerical analysis of seismic behavior of embankments founded on liquefiable soils, *Soils and Foundations*, **40**(2), 21–39.
73) Matsuoka, H., Suzuki, Y. and Murata, T. (1990): A constitutive model for soils evaluating principal stress rotation and its application to some deformation problems, *Soils and Foundations*, **30**(1), 142–154.
74) Modaressi, H. and Aubert, P. (1998): Element-free Galerkin

method for deforming multiphase porous media, *Int. J. Numer. Meth. Engrg*, 42, 313–340.
75) Moes, N., Dolbow, J. and Belytschko, T. (1999): A finite element method for crack growth without remeshing, *Int. J. Numer. Methods Eng.*, 46(1), 131–150.
76) Murakami, A., Setsuyasu, T. and Arimoto, S. (2005): Mesh-free method for soil-water coupled problem within finite strain and its numerical validity, *Soils and Foundations*, 45(2), 145–154.
77) Murakami, A., Nishimura, S., Fujisawa, K., Nakamura, K. and Higuchi, T. (2009): Data assimilation in geotechnical analysis using the particle filter, *Journal of Applied Mechanics*, 12, 99–105 (in Japanese).
78) Nagaoka, H., Yamazaki, M., Zhang, Y. and Okamura, T. (2001): Estimation of tow load-settlement relation of non-displacement piles based on back-analysis of in-situ tests, *Soils and Foundations*, 41(1), 39–55.
79) Nakai, T., Xu, L. and Yamazaki, H. (1997): 3D and 2D model tests and numerical analyses of settlements and earth pressures due to tunnel excavation, *Soils and Foundations*, 37(3), 31–42.
80) Nakai, T., Farias, M. M., Bastos, D. and Sato, Y. (2007): Simulation of conventional and inverted braced excavations using subloading t_{ij} Model, *Soils and Foundations*, 47(3), 597–612.
81) Namikawa, T., Koseki, J. and Suzuki, Y. (2007): Finite element analysis of lattice-shaped ground improvement by cement-mixing for liquefaction mitigation, *Soils and Foundations*, 47(3), 559–576.
82) Narita, K. and Ohne, Y. (1978): A study on the crack generation in fill-type dams, *Soils and Foundations*, 18(1), 11–24.
83) Neumann, S. P. (1973): Saturated-unsaturated seepage by finite elements, *Proc. ASCE*, 99(HY12), 2233–2250.
84) Newmark, N. M. (1959): A method of computation for structural dynamics, *Journal of Engineering Mechanics*, ASCE, 67–94.
85) Newmark, N. W. (1965): Effects of earthquakes on dams and embankments, *Fifth Rankine Lecture, Géotechnique*, 15, 139–159.
86) Nguyen, V. P., Rabczuk, T., Bordas, S. and Duflot, M. (2008): Meshless methods: A review and computer implementation aspects, *Mathematics and Computers in Simulation*, 79, 763–813.
87) Nishigaki, M., Futami, Y. and Kohno, I. (1986): An integrated finite difference method for seepage analysis in anisotropic aquifer, *Jour. of JSSMFE*, 26(3), 169–179 (in Japanese).
88) Nishimura, S., Shimada, K. and Fujii, H. (2002): Consolidation inverse analysis considering spatial variability and non-linearity of soil parameters, *Soils and Foundations*, 42(3), 45–61.
89) Nishimura, S., Nishiyama, T. and Murakami, A. (2005): Inverse analysis of soft grounds considering non-linearity and anisotropy, *Soils and Foundations*, 45(2), 87–96.
90) Noda, T., Asaoka, A. and Nakano, M. (2008): Soil-water coupled finite deformation analysis based on a rate-type equation of motion incorporating the SYS Cam-clay model, *Soils and Foundations*, 48(6), 771–790.
91) Noda, T., Takeuchi, H., Nakai, K. and Asaoka, A. (2009): Coseismic and post-seismic behavior of an alternately layered sand-clay ground and embankment system accompanied by soil disturbance, *Soils and Foundations*, 49(5), 739–756.
92) Nogami, T., Wang, W. and Wang, J.-G. (2004): Numerical method for consolidation analysis of lumpy clay fillings with meshless method, *Soils and Foundations*, 44(1), 125–142.
93) Ohtsuka, S., Yamada, E. and Matsuo, M. (1998): Stability analysis of earth structures resisting earthquake, *Soils and Foundations*, 38(1), 195–205.
94) Oka, F., Sekiguchi, K. and Goto, H. (1981): A method of analysis of earthquake-induced liquefaction of horizontally layered sand deposits, *Soils and Foundations*, 21(3), 1–17.
95) Oliaei, M. N., Soga, K. and Pak, A. (2008): Some numerical issues using element-free Galerkin mesh-less method for coupled hydro-mechanical problems, *Int. J. Numer. Anal. Meth. Geomech.*, 33(7), 915–938.
96) Onoue, A., Wakai, A., Ugai, K., Higuchi, K., Fukutake, K., Hotta, H., Kuroda, S. and Nagai, H. (2006): Slope failures at Yokowatashi and Nagaoka College of Technology due to the 2004 Niigata-ken Chuetsu Earthquake and their analytical considerations, *Soils and Foundations*, 46(6), 751–764.
97) Ortitz, M. and Simo, J. C. (1986): An analysis of a new class of iteration algorithms for elastoplastic constitutive relations, *Int. J. Numer. Methods Eng.*, 23, 353–336.
98) Pagano, L., Sica, S. and Coico, P. (2009): A study to evaluate the seismic response of road embankments, *Soils and Foundations*, 49(6), 909–920.
99) Pietruszczak, S. and Parvini, M. (2001): On limitations of a coupled dynamic analysis of saturated porous media, *Soils and Foundations*, 41(6), 153–156.
100) Pitilakis, K. and Moutsakis, A. (1989): Seismic analysis and behaviour of gravity retaining walls—The case of kalamata harbour quaywall, *Soils and Foundations*, 29(1), 1–17.
101) Poran, C. J. and Rodriguez, J. A. (1992): Finite element analysis of impact behavior of sand, *Soils and Foundations*, 32(4), 68–80.
102) Psarropoulos, P. N., Tazoh, T., Gazetas, G. and Apostolou, M. (2007): Linear and nonlinear valley amplification effects on seismic ground motion, *Soils and Foundations*, 47(5), 857–872.
103) Sakajo, S. and Kamei, T. (1996): Simplified deformation analysis for embankment foundation using elasto-plastic model, *Soils and Foundations*, 36(2), 1–11.
104) Sakaki, N., Nagaoka, H., Yokoyama, Y. and Okamoto, T. (1985): Dynamic analysis of underground cylindrical structures and comparison with results of vibration test and earthquake observation, *Soils and Foundations*, 25(3), 167–177 (in Japanese).
105) San, K. C., Leshchinsky, D. and Matsui, T. (1994): Geosynthetic reinforced slopes: limit equilibrium and finite element analyses, *Soils and Foundations*, 34(2), 79–85.
106) Sato, T. and Matsumaru, T. (2006): Numerical simulation of liquefaction and flow process using mesh free method, *Proc. JSCE*, 62(1), 22–34 (in Japanese).
107) Savvidou, C. and Britto, A. M. (1995): Numerical and experimental investigation of thermally induced effects in saturated clay, *Soils and Foundations*, 35(1), 37–44.
108) Shinoda, M., Horii, K., Yonezawa, T., Tateyama, M. and Koseki, J. (2006): Reliability-based seismic deformation analysis of reinforced soil slopes, *Soils and Foundations*, 46(4), 477–490.
109) Shogaki, T. and Kumagai, N. (2008): A slope stability analysis considering undrained strength anisotropy of natural clay deposits, *Soils and Foundations*, 48(6), 805–819.
110) Shoji, M. and Matsumoto, T. (1976): Consolidation of embankment foundation, *Soils and Foundations*, 16(1), 59–74.
111) Shoji, M., Ohta, H., Matsumoto, T. and Morikawa, S. (1989): Safety control of embankment foundation based on elastic-plastic back analysis, *Soils and Foundations*, 29(2), 112–126.
112) Shoji, M., Ohta, H., Arai, K., Matsumoto, T. and Takahashi, T. (1990): Two-dimensional consolidation back-analysis, *Soils and Foundations*, 30(2), 60–78.
113) Shuku, T., Murakami, A., Nishimura, S., Fujisawa, K. and Nakamura, K. (2010): Data assimilation of the settlement behavior of Kobe Airport constructed on reclaimed land using the particle filter, *Journal of Applied Mechanics*, 13, 67–78 (in Japanese).
114) Sica, S. and Pagano, L. (2009): Performance-based analysis of earth dams: Procedure and application to a sample case, *Soils and Foundations*, 49(6), 921–939.
115) Siddiquee, M. S. A., Tanaka, T., Tatsuoka, F., Tani, K. and Morimoto, T. (1999): Numerical simulation of bearing capacity characteristics of strip footing on sand, *Soils and Foundations*, 39(4), 93–109.
116) Simo, J. C. and Hughes, T. J. R. (1998): *Computational Inelasticity; Interdisciplinary Applied Mathematics*, Springer.
117) Tanaka, T. and Sakai, T. (1993): Progressive failure and scale effect of trap-door problems with granular materials, *Soils and Foundations*, 33(1), 11–22.
118) Tani, S., Tsukuni, S. and Shiomi, T. (2009): Performance of a fill dam based on the performance-based design concept and study of a seismic retrofitting method, *Soils and Foundations*, 49(6), 841–851.
119) Taniguchi, E., Whitman, R. V. and Marr, W. A. (1983): Predic-

tion of earthquake-induced deformation of earth dams, *Soils and Foundations*, 23(4), 126–132.
120) Tikhonov, A. N. (1963): Solution of incorrectly formulated problems and the regularization method, *Soviet Mathematics Doklady*, 4, 1035–1038.
121) Tokimatsu, K. and Sekiguchi, T. (2006): Effects of nonlinear properties of surface soils on strong ground motions recorded in Ojiya during 2004 Mid Niigata Prefecture Earthquake, *Soils and Foundations*, 46(6), 765–776.
122) Tosaka, N. and Utani, A. (1993): New filter theory-Boundary element method and its application to inverse problems, *Inverse Problems in Engineering Mechanics*, (eds. by Bui and Tanaka), 453–460.
123) Toyota, H., Nakamura, K. and Sakai, N. (2006): Evaluation of dike and natural slope failure induced by heavy rainfall in Niigata on 13 July 2004, *Soils and Foundations*, 46(1), 83–98.
124) Ugai, K. (1989): A method of calculation of total safety factor of slope by elasto-plastic FEM, *Jour. of JSSMFE*, 29(2), 190–195 (in Japanese).
125) Ugai, K. and Leshchinsky, D. (1995): Three-dimensional limit equilibrium and finite element analyses: a comparison of results, *Soils and Foundations*, 35(4), 1–7.
126) Wakai, A. and Ugai, K. (2004): A simple constitutive model for the seismic analysis of slopes and its applications, *Soils and Foundations*, 44(4), 83–98.
127) Wakai, A., Ugai, K., Onoue, A., Kuroda, S. and Higuchi, K. (2010): Numerical modeling of an earthquake-induced landslide considering the strain-softening characteristics at the bedding plane, *Soils and Foundations*, 50(4), 515–527.
128) Wang, J.-G., Liu, G. R. and Lin, P. (2001): A point interpolation method for simulating dissipation process of consolidation, *Comp. Methods Appl. Mech. Engrg.*, 190, 5907–5922.
129) Watanabe, H. and Kawakami, T. (1995): Characteristics of elementary dynamic behavior for three dimensional seismic response of a fill dam, *Soils and Foundations*, 35(1), 45–54.
130) Wei, W. B. and Cheng, Y. M. (2010): Stability analysis of slope with water flow by strength reduction method, *Soils and Foundations*, 50(1), 83–92.
131) Wu, C.-T., Chen, J.-S., Chi, L. and Huck, F. (2001): Lagrangian meshfree formulation for analysis of geotechnical materials, *J. Engrg. Mech., ASCE*, 127(5), 440–449.
132) Yashima, A., Leroueil, S., Oka, F. and Guntoro, I. (1998): Modelling temperature and strain rate dependent behavior of clays: one dimensional consolidation, *Soils and Foundations*, 38(2), 63–73.
133) Yatomi, C., Yashima, A., Iizuka, A. and Sano, I. (1989): Shear bands formation numerically simulated by a non-coaxial cam-clay model, *Soils and Foundations*, 29(4), 1–13.
134) Ye, G., Zhang, F., Yashima, A., Sumi, T. and Ikemura, T. (2005): Numerical analysis on progressive failure of slope due to heavy rain with 2D and 3D FEM, *Soils and Foundations*, 45(2), 1–16.
135) Zhang, F. and Kimura, M. (2002): Numerical prediction of the dynamic behaviors of an RC group-pile foundation, *Soils and Foundations*, 42(3), 77–92.
136) Zhang, F., Yashima, A., Osaki, H., Adachi, T. and Oka, F. (2003): Numerical simulation of progressive failure in cut slope of soft rock using a soil-water coupled finite element analysis, *Soils and Foundations*, 43(5), 119–131.
137) Zheng, H., Zhou, C. B. and Liu, D. (2009): A robust solution procedure for the rigorous methods of slices, *Soils and Foundations*, 49(4), 537–543.
138) Zienkiewicz, O. C., Humpheson, C. and Lewis, R. W. (1975): Associated and non-associated visco-plasticity and plasticity in soil mechanics, *Géotechnique*, 25(4), 671–689.
139) Zienkiewicz, O. C. and Shiomi, T. (1984): Dynamic behaviour of saturated porous medium: the generalized Biot formulation and its numerical solution, *Int. J. Numer. Anal. Meth. Geomech.*, 8, 71–96.
140) Zornberg, J. G. and Kavazanjian, E. Jr. (2001): Predication of the performance of a geogrid-reinforced slope founded on solid waste, *Soils and Foundations*, 41(6), 1–16.